

Computational Study of ZSWCNTs and ZSWBNNTs as a Career Different Anticancer Drug

Mohammed Hamid Neamah¹, Mohammed H. Mohammed^{1,2,3,*}

¹Department of Physics, College of Science, University of Thi-Qar, Nassiriya, Iraq

²Department of Medical Physics, College of Applied medical Science, Shatrah University, Thi-Qar, Iraq.

³ Department of Physics, College of Science, Southern Illinois University, Carbondale, USA

*Corresponding author: mohammedhalol@shu.edu.iq & mohammedph20@sci.utq.edu.iq & mohammedph14@gmail.com

Abstract:

We utilize the ZSWCNTs and ZSWBNNTs as a career to (CH, CY, and 5-FU) anticancer drugs. DFT method is utilized to study various electronic properties of the adsorption of these anticancer drugs on ZSWCNTs and ZSWBNNTs. The results are pointed out that these tubes have semiconductor behaviors and the electronic band gap is increasing with increasing the diameter of the tube, excepted the (6,0) ZSWCNTs has a metal behavior with zero electronic band gap. Due to the total energy is increasing with increasing the diameter, these tubes become more stable and lower reactive. Results shown that the complex structures have electronic band gap less than the pristine of these tubes. By adsorbing the same anticancer drug on the ZSWCNTs and ZSWBNNTs, we found out that the complex structures (anticancer drug/ZSWBNNTs) have interesting results compared with the complex structures anticancer drug/ZSWCNTs. So, the electronic band gap is reduced for complex structure compared with pristine tubes. Also, the anticancer drug/ZSWBNNTs is more stable compared with anticancer drug/ZSWCNTs. The adsorption energy is increasing by increasing the diameter of tube with anticancer drug, except the 5-FU/(7,0) ZSWBNNTs has an opposite behavior. Then, we recognized that the CH/(11,0) ZSWBNNTs are the best substrate to carrier the anticancer drug, due to it has a higher value of the adsorption energy Eads compared to others. In brief, we detected that the ZSWBNNTs is the best substrate to deliver these anticancer drugs compared with ZSWCNTs.

Keywords: electronic band gap; adsorption energy; DFT methods; anticancer drug; ZSWCNTs; ZSWBNNTs

دراسة حسابية لـ ZSWCNTs و ZSWBNNTs كناقل لأنواع مختلفة من ادوية السرطان

محمد حميد نعيمه¹، محمد هلول محمد^{1,2,3}

¹قسم الفيزياء، كلية العلوم، جامعة ذي قار، الناصرية، العراق

²قسم الفيزياء الطبية، كلية العلوم الطبية التطبيقية، جامعة الشطرة، ذي قار، العراق.

³قسم الفيزياء، كلية العلوم، جامعة جنوب إلينوي، كاربونديل، إلينوي، الولايات المتحدة الأمريكية

الخلاصة:

تم استخدام أنابيب الكربون النانوية ZSWCNTs وأنابيب الكربون النانوية ZSWBNNTs كناقل لأدوية السرطان (CH و CY و 5-FU). يتم استخدام طريقة DFT لدراسة الخصائص الإلكترونية المختلفة لامتصاص هذه الأدوية المضادة للسرطان على أنابيب الكربون النانوية ZSWCNTs وأنابيب الكربون النانوية ZSWBNNTs. تشير النتائج إلى أن هذه الأنابيب لها سلوك أشباه الموصلات وأن الفجوة النطاقية الإلكترونية تتزايد مع زيادة قطر الأنبوب، باستثناء أنابيب الكربون النانوية ZSWCNTs (6,0) التي لها سلوك معدني مع فجوة نطاقية إلكترونية صفرية. نظرًا لزيادة الطاقة الكلية مع زيادة القطر، تصبح هذه الأنابيب أكثر استقرارًا وأقل تفاعلية. أظهرت النتائج أن الهياكل المعقدة لها فجوة نطاقية إلكترونية أقل من الأصل لهذه الأنابيب. من خلال امتصاص نفس الدواء المضاد للسرطان على أنابيب الكربون النانوية ZSWCNTs وأنابيب الكربون النانوية ZSWBNNTs، وجدنا أن الهياكل المعقدة (دواء مضاد للسرطان/أنابيب الكربون النانوية ZSWBNNTs) لها نتائج مثيرة للاهتمام مقارنة بالهياكل المعقدة لدواء مضاد للسرطان/أنابيب الكربون النانوية ZSWCNTs. لذا، يتم تقليل فجوة النطاق الإلكتروني للبنية المعقدة مقارنة بالأنابيب البكر. أيضًا، يكون عقار السرطان ZSWBNNTs أكثر استقرارًا مقارنة بعقار السرطان ZSWCNTs. تزداد طاقة الامتصاص بزيادة قطر الأنبوب مع عقار السرطان، باستثناء أن 5-FU/(7,0) ZSWBNNTs لها سلوك معاكس. بعد ذلك، أدركنا أن CH/(11,0) ZSWBNNTs هي أفضل ركيزة لحمل عقار السرطان، نظرًا لأنها تتمتع بقيمة أعلى لطاقة الامتصاص Eads مقارنة بالآخرين. باختصار، اكتشفنا أن ZSWBNNTs هي أفضل ركيزة لتوصيل هذه الأدوية المضادة للسرطان مقارنة بـ ZSWCNTs.

1. Introduction

Carbon Nanotubes are carbon-based compounds that resemble tubes and have nanometer-sized diameters. Their distinctive structure, which resembles a rolled-up hexagonal mesh, is developed from graphite sheets. The carbon nanotubes are of two types namely: Single-walled carbon nanotubes (SWCNTs) and multi-walled carbon nanotubes (MWCNTs). SWCNTs can be formed in three different designs: armchair SWCNTs when ($m = n$), chiral SWCNTs when ($n \neq m$), and zigzag SWCNTs when ($n, m = 0$); where n and m represent the number of unit vectors along circumferential direction. The design depends on the way the graphene is wrapped into a cylinder. MWCNTs consist of several coaxial cylinders, each made of a single graphene sheet surrounding a hollow core[1, 2]. The exceptional qualities of SWCNTs are one of its primary traits. They have great thermal conductivity, high flexibility, and low density. They are also chemically inert, which makes them excellent for a variety of uses in the disciplines of materials science, electronics, optics, and nanotechnology. Due to their potential as anticancer drug carriers, SWCNTs have attracted a lot of attention in biomedical science lately[3]. Enhancing SWCNTs' solubility and compatibility with biological systems is largely dependent on surface functionalization. Targeted medication delivery or immune recognition for therapeutic effects are made possible by the ZSWCNTs by attaching or adsorbing active compounds to their surfaces. SWCNTs have additionally demonstrated antibacterial and antifungal properties[4].

Zigzag single-wall Boron nitride nanotubes (ZSWBNNTs), in addition to ZSWCNTs, are another kind of nanostructure that has drawn attention for use in biological applications. High elastic and tensile strength, as well as exceptional high-temperature oxidation resistance, are all characteristics of SWBNNTs. Additionally, they exhibit strong insulation and thermal stability qualities. Since ZSWBNNTs are non-toxic in comparison to ZSWCNTs, they can be used in biological applications[5].

Antimetabolite chemotherapeutic are widely used to employ their anticancer effects, typically over non-specific cytotoxic effects. Contrariwise, the patients vary intensely with esteem to treatment result, and the sources of heterogeneity stay mostly unknown [6]. There are many types of the antimetabolites drugs such as [5-fluorouracil (5-FU), hydroxyurea(HU), and chlorambucil (CH)], which have utilized to treat the human body from various diseases, such as rheumatologic disorder, lymphoblastic, cancer and leukemia.

5-FU anticancer drug is an antimetabolite commonly used in chemotherapy treatment regimens for various types of cancers like colorectal cancer It functions by blocking thymidylateel synthase, an enzyme necessary for the synthesis of DNA. The trade name of the 5-FU is adrucil, carac, efudex, and fluoriplex. The chemical formula of the 5-FU is $C_4H_3FN_2O_2$. Fluorouracil administration presents challenges, including limited tumor-specific uptake and rapid metabolism, despite its effectiveness in certain cases. Because they increase drug stability, allow for controlled release, and improve targeted delivery to cancer cells, carbon nanotube-based drug delivery systems present a viable remedy[7].

CY anticancer drug is one of several clinically important cancer drugs whose therapeutic efficacy is due in part to their ability to stimulate antitumor immune responses. The

chemical formula of the CY anticancer is $C_7H_{15}Cl_2N_2O_2P$. CY is widely used as an anticancer drug and routinely used as a regimen for hemopoietic stem cell transplant[8]. CY may also be used to prepare the host for immunotherapy due to its immunosuppressive properties. Research has shown that administering CY increased the number of dendritic cells, which in turn stimulated the immune response by encouraging the mobilization of hematopoietic stem cells and driving the immune response directly. In spite of its many positive effects, CY has been linked to a number of negative side effects, including pneumonia, pulmonary fibrosis, suppression of bone marrow, induction of genotoxicity, and heart toxicity. Here, the CY injection could serve as our study's experimental model[9].

Alkylating agents have received far too much attention in the field of cancer therapy in recent years. Nitrogen mustard CH, one of the many varieties of alkylating agents, is a well-known example of a bifunctional alkylating agent as an anticancer medication that has already received approval for the treatment of cancer. The chemical formula of the CH anticancer is $C_{14}H_{19}Cl_2NO_2$. Long recognized for its high toxicity and tumor activity, CH is used to treat chronic lymphocytic leukemia. However, it can also be used to treat other tumors, including ovarian carcinoma, trophoblastic neoplasm, and some non-Hodgkin lymphoma forms. Currently, there is a lot of interest in polymeric prodrugs because of their potential for drug delivery to cancer cells and low toxicity [10].

To increase the specificity of cancer treatment during chemotherapy, drug delivery systems incorporating SWBNNTs have been created. SWBNNTs enhance the circulatory transit of several medications by increasing their water solubility, such as 5-FU. It has been demonstrated that the electrical characteristics of the drug molecules are altered by their interaction with SWBNNTs, offering helpful information for the experimental stages[5].

One of the most difficult problems that a medicine delivery technique can solve is cancer. The word "cancer" refers to a group of chronic illnesses that vary widely in kind and location but have the feature of aberrant cells proliferating uncontrollably. Chemotherapy is widely utilized in the treatment of cancer, but several potential negative side effects of anti-cancer medications employed in this therapeutic method, such as toxic side effects on rapidly proliferating healthy cells and multidrug resistance, would limit their continued use in the treatment of cancer. In this regard, nanoscale delivery systems have been developed to combat chemotherapy-assisted therapeutics by delaying drug resistance, providing sustained and targeted drug release into the tumor microenvironment, facilitating the drug's penetration into cancer cells and tissues, protecting the drug from harmful reactions, oxidation, and environmental stress, and more importantly, reducing the amount of the drug that must be administered[11]. The association of anticancer drugs to delivery systems has been an interesting approach to selectively delivering these active agents and, at the same time, reducing their toxicity[11].

In recap, SWCNTs and SWBNNTs have special qualities that make them interesting candidates for a range of biomedical applications. Their usefulness in medicine administration, sensing, water treatment, and other areas is a result of their tubular structure and excellent mechanical and electrical qualities. Carbon nanotubes have a significant deal of potential to transform targeted drug delivery and cancer therapy with additional study and development[12].

A few of SWCNTs with theoretical backgrounds have vast knowledge of medical drug delivery methods. CNTs have been researched extensively in pharmaceutical medication delivery systems. The use of the SWCNTs as drug carriers can lead to a number of biochemical issues regarding the interactions between drug molecules and SWCNTs. Numerous theoretical and experimental studies have been conducted on this topic. Moreover, minimal toxicity was demonstrated when using carbon nanotubes as medication carriers. While carbon nanotubes can be either metallic or semiconductor, depending on their diameter and chirality, boron nitride nanotubes are semiconductors. Moreover, SWBNNTs have been the subject of theoretical research due to their high bonding energy and inherent non-cytotoxicity. Soltani et al. used the straightforward cancer medication 5-fluorouracil (5-FU) for localized drug delivery. Despite reports of strong adsorption on metal-doped SWBNNTs, they demonstrated that the adsorption type of 5-FU (O- and F-sides) on the pristine (8,0) are electrostatic in nature[7]. There are still significant gaps in the information despite this study.

2. Computational Details

In this study, DFT [13, 14] calculations that were implemented in the Gaussian 09 package [15-19] with the basis set B3LYP/6-31G were used to optimize the structure of ZSWCNTs and ZSWBNNTs. We actually selected this basis set because it is adequate for related geometry optimizations of this molecule. The relaxing of the molecular structures was the first step in our computation. After that, we looked at the molecules' electronic properties

The highest-occupied molecular orbital (E_{HOMO}) and lowest-unoccupied molecular orbital (E_{LUMO}) energies were also examined. The following relationships were used to compute the electronic band gap and Fermi level energy[20-27]:

$$E_{gap} = E_{LUMO} - E_{HOMO} \quad (1)$$

$$E_{Fl} = (E_{HOMO} - E_{LUMO}) / 2 \quad (2)$$

$$E_{ads} = E_{complex\ structure} - (E_{pristine\ CNTs\ or\ BNNTs} + E_{anticancer\ drug}) \quad (3)$$

Where the $E_{complex\ structure}$, and $E_{pristine\ CNTs\ or\ BNNTs}$ anticancer drug indicate to the total energy of the anticancer drugs/(ZSWCNTs or SWBNNTs), the total energy of the pristine CNTs or SWBNNTs, and the total energy of the anticancer drug, respectively [28, 29].

According to the DFT method and Koopmans' theorem, we studied the reactivity of these anticancer drugs on the substrate (ZSWCNTs and ZSWBNNTs) via computing the next parameters [14, 28, 30]:

$$I_P = -E_{HOMO} \quad (4)$$

$$E_A = -E_{LUMO} \quad (5)$$

$$H = (I_P - E_A)/2 \quad (6)$$

$$S = \frac{1}{2H} \quad (7)$$

$$\mu = (I_P + E_A)/2 \quad (8)$$

$$\omega = \frac{\mu^2}{2H} \quad (9)$$

Where I_P , E_A , H , S , μ , and ω are indicated the ionization potential, chemical hardness, chemical softness, chemical potential, electronegativity, and electrophilicity index, consecutively [31, 32].

After that, we investigated that how can utilize the ZSWCNTs and ZSWBNNTs structure to carry these anticancer drugs by putting this anticancer drug upon the slab of the ZSWCNTs and SWBNNTs [33, 34].

3. Results and Discussion

3.1. The structural and electronic properties of the pristine ZSWCNTs and ZSWBNNTs

Firstly, all geometrical structures are optimized by using DFT method, as displayed in Figs. 1 and 2. So, we pointed out that the bond length between C-C and B-N is 1.42 Å, respectively, which is very comfortable with previous studies [19, 35, 36]. By computing the electronic band structures of all tubes, we detected that the (6,0) ZSWCNTs has a metallic behavior with electronic band gap is zero at Fermi level, as pointed out in Fig.3. However, the ((7,0), (11,0) ZSWCNTs) and ((6,0), (7,0), and (11,0) ZSWBNNTs) have semiconductor behaviors, as shown in Figs. 3 and 4. So, all these results are in agreement with preceding references [37-39].

The electronic band structure of the (6 or 7 or 11,0) ZSWCNTs are shown in Fig. 3. We detected that the electronic band gap of the (6,0) ZSWCNTs is zero, as pointed out in Fig. 3(a), which led to have a metallic behavior. However, the behavior of the (7,0) and (11,0) ZSWCNTs are semiconductor behaviors with very small value of the electronic band gap at r point, as shown in Fig. 3 (b and c). So, these results are very comfortable with previous studies [40-42]. For stability, the results shown that the stability is increased by increasing the diameter of these tube due to the total energy is increased by increasing the diameter of the tube (see Table 1). Also, the results exhibited that the Fermi level is reduced by increasing the diameter of the tube, as presented in Table 1.

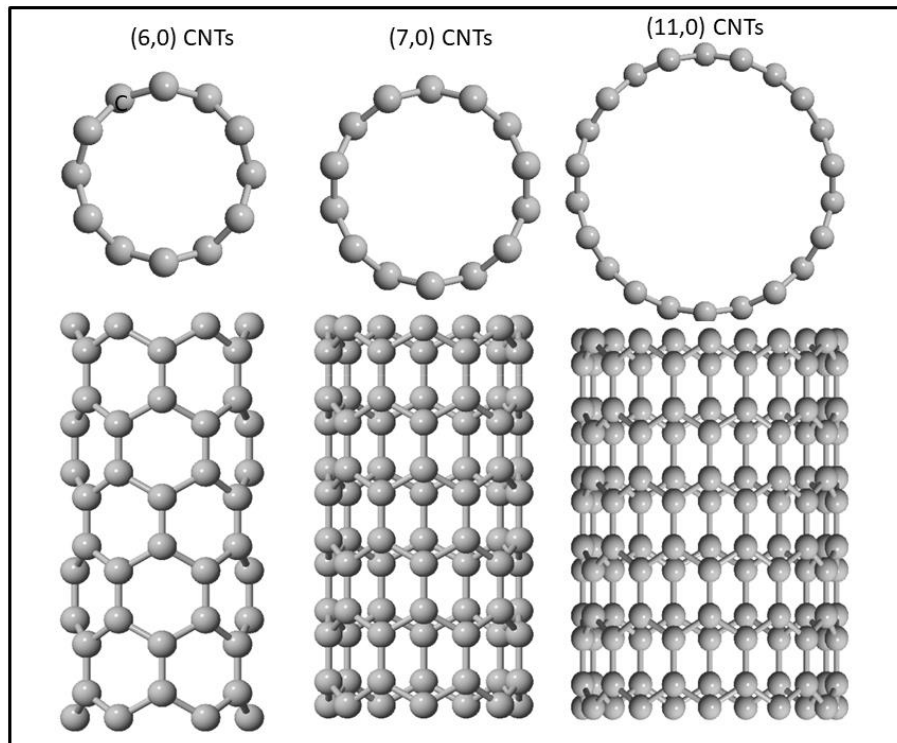


Figure- 1 The optimization structure of the ZSWCNTs

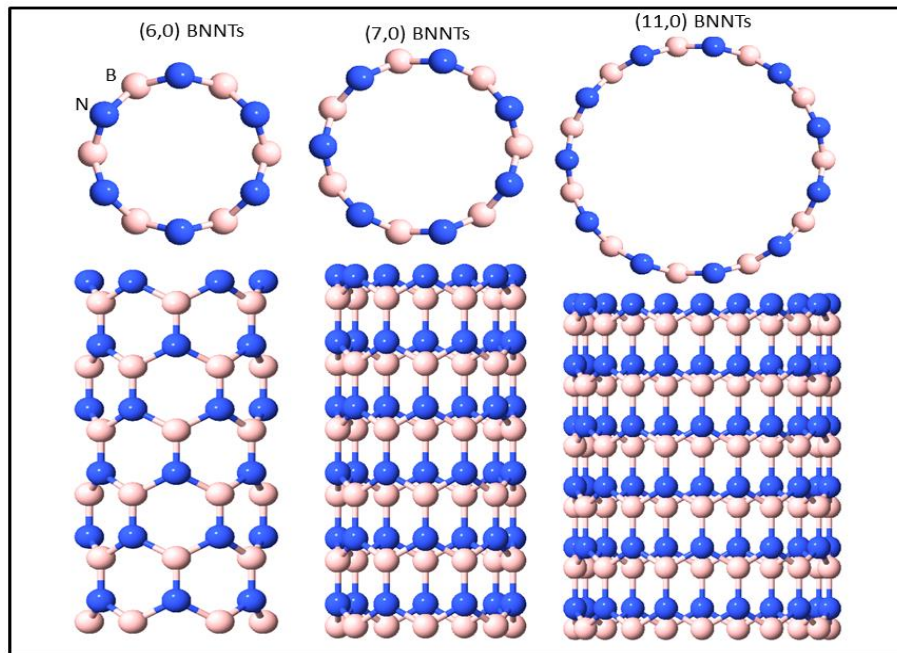


Figure- 2 The optimization structure of the ZSWBNNTs.

The electronic band structure of the (6 or 7 or 11,0) ZSWBNNTs are shown in Fig. 4. We detected that the electronic band gap of the (6,0) and (7,0) ZSWBNNTs is (2.635-3.337) eV, respectively, as pointed out in Fig.4, which led to make them semiconductor behaviors, as represented in Fig. 4(a and b). For (11,0) ZSWBNNTs, has an insulator behavior with greater value of the electronic band gap, as shown in Fig. 4(c). So, these

results are very comfortable with previous studied [43]. For stability, the results showed that the stability is increased by increasing the diameter of these tube. Moreover, the results exhibited that the Fermi level is reduced by increasing the diameter of the tube except the (7,0) has an opposite behavior, as presented in Table 1.

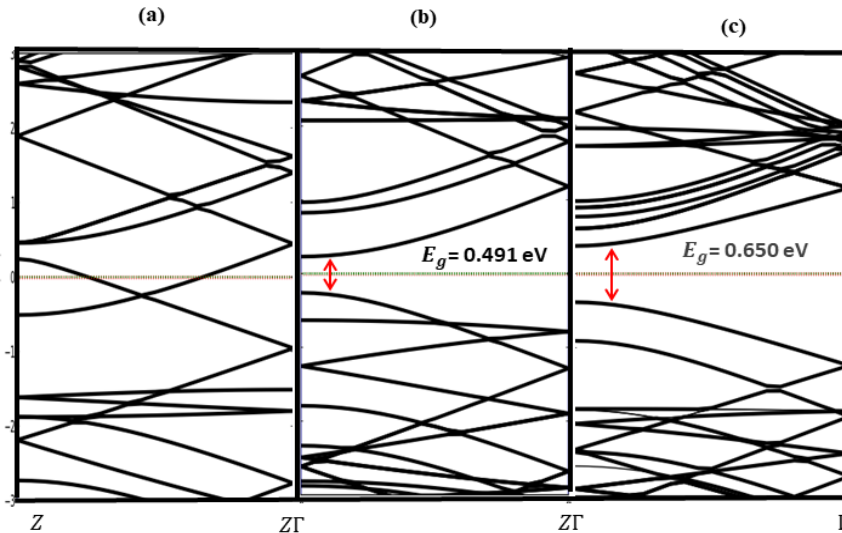


Figure - 3 The electronic band structure of the ZSWCNTs: (a) for (6,0), (b) for (7,0), and (c) for (11,0)

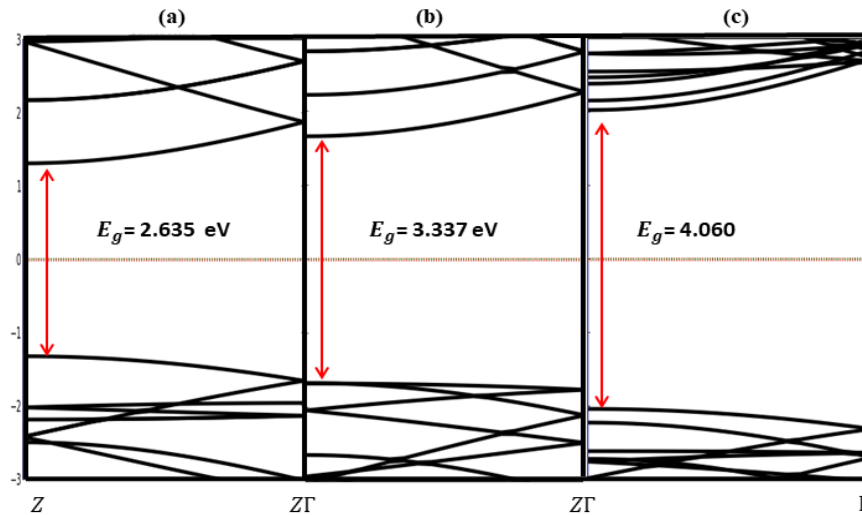


Figure -4 The electronic band structure of the ZSWBNTs: (a) for (6,0), (b) for (7,0), and (c) for (11,0)

Table 1- Some electronic properties of the different tubes; the electronic band gap (E_{gap}), exchange-correlation energy (E_{exc}), kinetic energy (E_k), (E_{EL}) electrostatics energy, (E_T) total energy, and (E_{FL}) Fermi level energy

System	$E_{gap}(eV)$	$E_{exc}(eV)$	$E_k(eV)$	$E_{EL}(eV)$	$E_T(eV)$	$E_{FL}(eV)$
(6,0) ZSWCNTs	0.000	-3673.288	7963.463	-15631.916	-11341.766	-4.132
(7,0) ZSWCNTs	0.491	-4281.570	9274.113	-18232.844	-13240.302	-4.372
(11,0) ZSWCNTs	4.065	-6716.689	14513.722	-28624.259	-20827.227	-3.983
(6,0) ZSWBNTs	2.635	-3826.006	9059.245	-17974.210	-12740.971	-4.270
(7,0) ZSWBNTs	3.337	-4458.927	10548.402	-20961.037	-14871.562	-4.253
(11,0) ZSWBNTs	4.060	-6995.253	16526.595	-32918.485	-23387.143	-3.894

3.2 The Electronic properties of the anticancer drugs

By using DFT calculations, the geometrical structures of all anticancer drugs (CH, CY, and 5-FU) are thoroughly optimized, as pointed out in Fig.5. Initially, we calculated the total energy of all these anticancer drugs to examine the stability of these anticancer drugs. We revealed that the CY molecule has a larger total energy value compared with other molecules, which led to make less reactive and more stable, as seen in Table 2. Additionally, the CY anticancer drug has a semiconductor behavior, but the 5-FU and CH have insulator behaviors, as demonstrated in Table 2. The Fermi level (EFL) is seated at zero point, which is the middle point of the HOMO and LUMO energies.

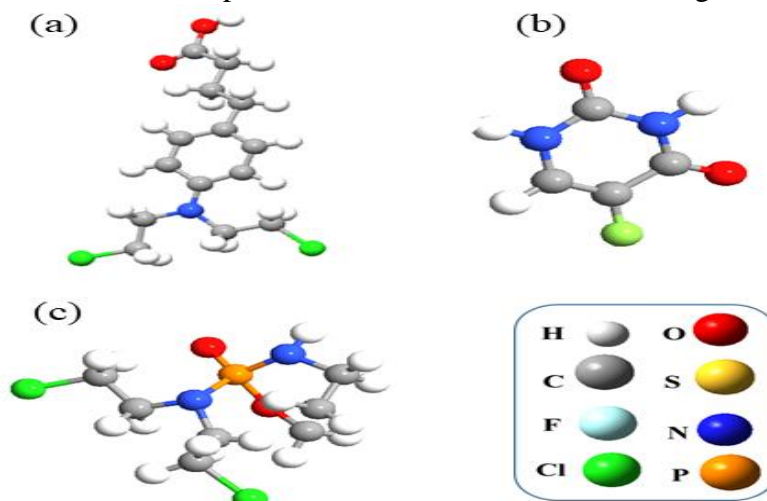


Figure -5 The geometrical structures of the anticancer drugs, (a) CH , (b) 5-FU and (c) CY

Table 2- The electronic properties of the various anticancer drugs.

Anticancer drugs	E_T (eV)	α (Debye)	E_{HOMO} (eV)	E_{LUMO} (eV)	E_{Gap} (eV)	E_{FL} (eV)
Cyclophosphamide (CY)	- 48846.547	7.270	-3.724	-1.391	2.334	-2.558
5-Fluorouracil (5-FU)	- 13980.083	5.196	-7.459	-2.762	4.697	-5.111
Chlorambucil (CH)	- 45426.298	1.893	-4.973	-0.436	4.537	- 2.7045

3.3. The electronic properties of (n,0) ZSWCNTs and ZSWBNNTs with anticancer drugs.

After we computed various electronic properties of the pristine ZSWCNTs, ZSWBNNTs, and anticancer drugs. We investigated different electronic properties of the complex structures (anticancer drug/(ZSWCNTs or ZSWBNNTs)) in different location of the anticancer drugs. So, the electronic band structure of the CY/(6,0) ZSWCNTs and CY/(6,0) ZSWBNNTs are computed, as displayed in Fig. 6. Our finding shown that the CY/(6,0) ZSWCNTs has a metallic behavior with zero electronic band gap, as shown in

Fig. 7 (a). While the CY/(6,0) ZSWBNNTs has a semiconducting behavior with a direct transition of electrons at the Γ point, and the electronic band gap energy is 2.433eV, as displayed in Fig.7 (b). The total energy is computed from the sum of the (kinetic, electrostatic, and exchange-correlation) energies in order to study the stability of the complex structures. We detected that the total energy is increased by increasing the diameter of the tube, which is utilized as a carrier to anticancer drug. However, the total energy of the anticancer drug/ZSWBNNTs has a higher value of the total energy of the anticancer drug/ZSWCNTs, which led to make the anticancer drug/ZSWBNNTs more stable and lower reactive, as displayed in Table 3..Also, the Fermi level of the anticancer drug/ZSWBNNTs is shifted down compared anticancer drug/ZSWCNTs (see Table 3).

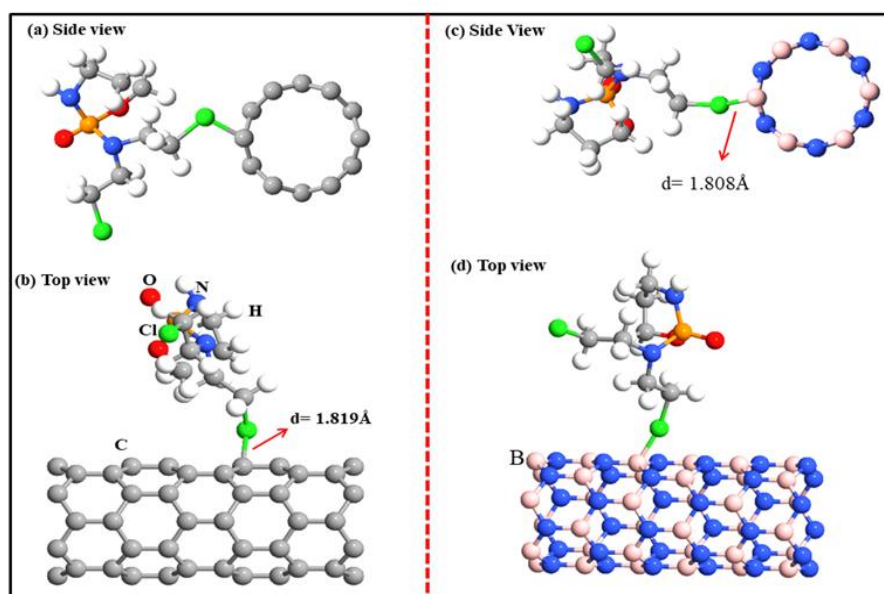


Figure -6 The geometrical structure of the CY/ (6,0) ZSWCNTs (a and b) and CY/ (6,0) ZSWBNNTs (c and d)

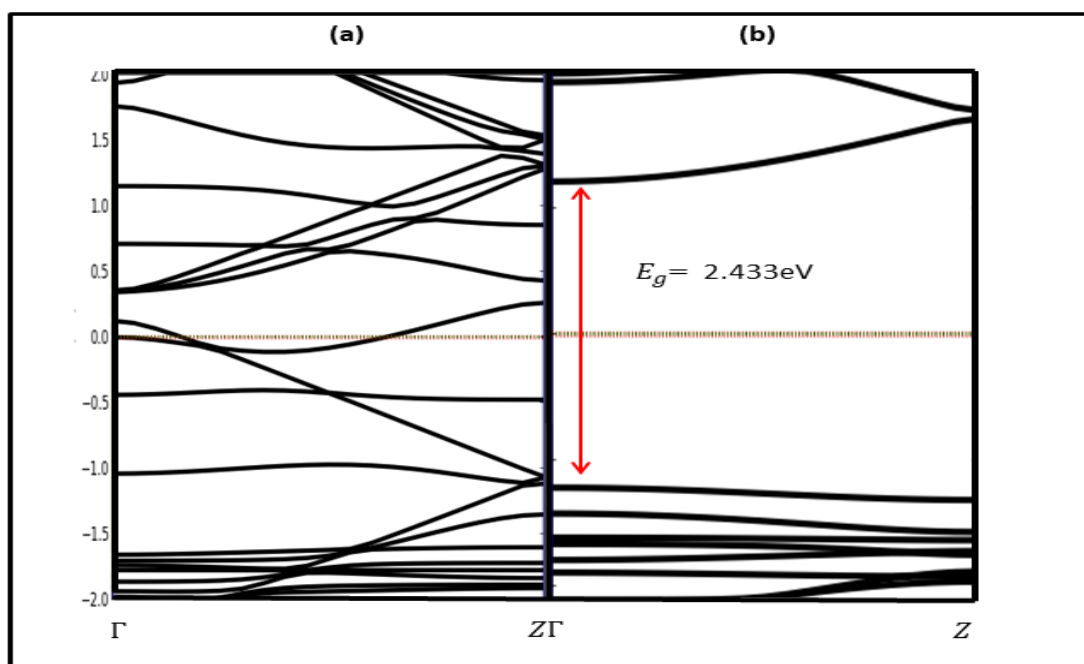


Figure -7 The electronic band structure of the (a) CY/(6,0) ZSWCNTs and (b) CY/(6,0) ZSWBNNTs

The electronic properties of the 5-FU/(7,0)ZSWCNTs and 5-FU/ZSWBNNTs are investigated. We started by optimization the geometrical structures of these complex structures, as showed in Fig. 8. Our finding demonstrated that these complex structures have semiconductor behaviors with direct electronic transition from valence to conduction bands at Γ point, as represented in Fig. 9. Also, we detected that electronic band gap and total energy have higher values in the 5-FU/ZSWBNNTs compared to 5-FU/ZSWCNTs, as presented in Table 3. Additionally, The Fermi level value is shifted down for 5-FU/ZSWBNNTs compared with the 5-FU/ZSWCNTs, as publicized in Table 3.

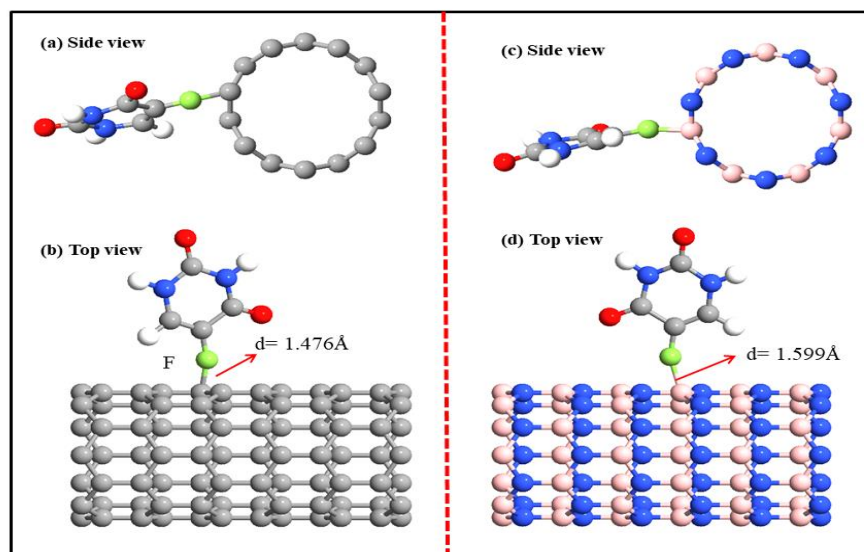


Figure -8 The optimization structures of the 5-FU/ (7,0) ZSWCNTs (a and b) and 5-FU/ (7,0) ZSWBNNTs (c and d)

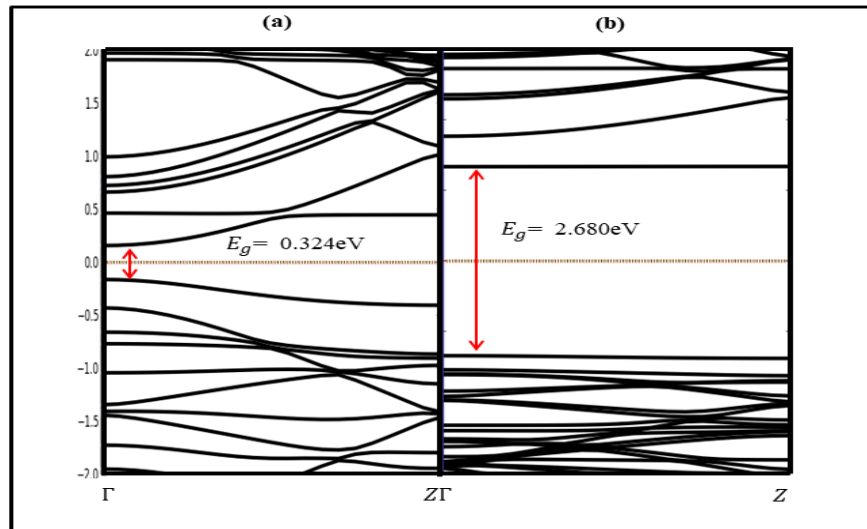


Figure - 9 The electronic band structure of the (a) 5-FU/(7,0) ZSWCNTs and (b)5-FU/(7,0) ZSWBNNTs

After that we computed some electronic properties of the complex structure (CH/(11,0) ZSWCNTs and CH/(11,0)ZSWBNNTs). These complex structures are optimized, as exposed in Fig. 10. Our finding demonstrated that the CH/(11,0) ZSWCNTs have semiconductor behaviors (see Fig. 11(a)) with direct electronic transition from valence to conduction bands at Γ point while the CH/(11,0) ZSWBNNTs has a semimetal behavior with electronic band gap is 0.056 eV, as represented in Fig. 11 (b). Also, we detected that electronic band gap and total energy of the CH/(11,0) ZSWBNNTs have higher values compared with CH/(11,0)ZSWCNTs, as mentioned in Table 3.

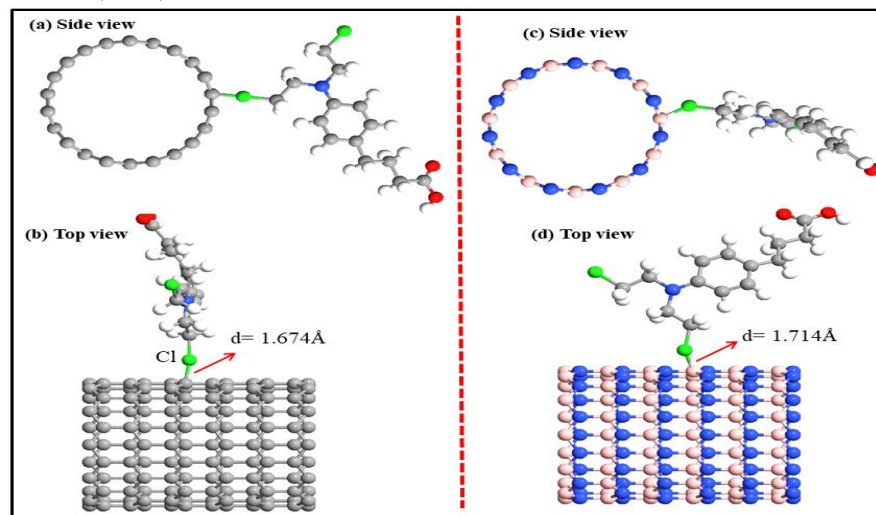


Figure -10 The geometrical structure of the CH/ (11,0) ZSWCNTs (a and b) and CH/ (11,0) ZSWBNNTs (c and d)

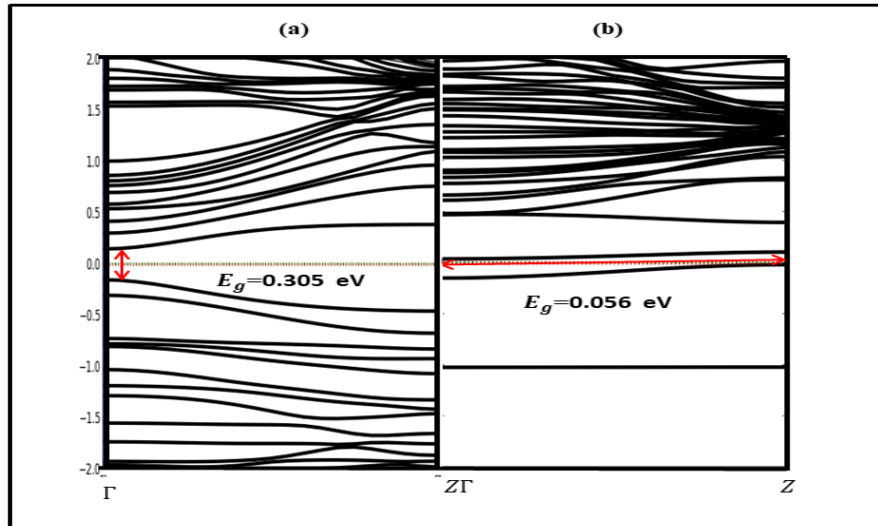


Figure -11 The electronic band structure of the (a) CH/(11,0) ZSWCNTs and (b) CH/(11,0) ZSWBNTs.

Table 3- Some electronic properties of the complex structures; the electronic band gap (E_{gap}), exchange-correlation energy (E_{exc}), kinetic energy (E_k), electrostatic energy (E_{EL}), Total energy (E_T), and Fermi level energy (E_{FL}).

System	E_{gap} (eV)	E_{exc} (eV)	E_k (eV)	E_{EL} (eV)	E_T (eV)	E_{FL} (eV)
CY/(6,0) ZSWCNTs	0.000	-4916.597	10349.742	-20699.314	-15266.197	-3.871
CY/ (6,0) SWBNTs	2.433	-5069.630	11445.217	-23045.379	-16669.791	-4.097
5- FU / (7,0)ZSWCNTs	0.325	-4978.282	11202.468	-22187.756	-15963.570	-3.884
5-FU/(7,0) SWBNTs	2.680	-5149.898	12449.782	-24901.293	-17601.409	-4.157
CH/ (11,0) SWCNTs	0.305	-8168.835	17564.496	-34760.717	-25365.057	-3.712
CH/ (11,0) SWBNTs	0.056	-8522.046	19993.361	-39160.717	-27689.511	-2.257

We also found the adsorption energy (E_{ads}) is increasing by increasing the diameter of the complex structures, except the 5- FU/(7,0)ZSWBNTs has an opposite behavior, as represented in Table 4.

Table 4- The adsorption energy of the complex structures.

System	E_{ads} (eV)
CY/ (6,0) ZSWZCNTs	-6.698
5-FU/ (7,0) ZSWZCNTs	-8.011
CH/ (11,0) ZSWZCNTs	-22.994
CY/ (6,0) ZSWZBNTs	-2.309
5-FU/ (7,0) ZSWZBNTs	-1.432
CH/ (11,0)S ZSWZBNTs	-258.456

3.4. The global reactivity of the complex structures

Based on the Koopmans' theorem, we discovered that the ZSWCNTs and ZSWBNNTs have very small μ values, which resulted in a decreased level of chemical reactivity. All complex structures have smaller value of the μ , which led to make these complex structures have lower reactive, as represented in Table 5. Also, the results shown that the CH/(11,0)ZSWBNNTs has a smaller value of the IP compared with others structures, which led to a higher ability to donate the electrons and became action comparison with complex structures, as displayed in Table 5. The (11,0)ZSWBNNTs have a higher value of the H, comparison with all structures, which is referred to lower ability to transfer an electron. Then, they required a higher exaction energy to transfer electrons, as mentioned in Table 5. Additionally, the S is reduced by increasing the diameter in the all complex structures, except the CH/(11,0) ZSWBNNTs has an opposite behavior. So, this result is very comfortable with result is shown in Table 5.

Table 5- The Global chemical indexes of the ZSWCNTs, ZSWBNNTs, and complex structures

System	μ (eV)	I_P (eV)	E_A (eV)	H (eV)	S (eV)	ω (eV)
(6,0)ZSWCNTs	-	-	-	-	-	-
(7,0)ZSWCNTs	0.007	0.251	-0.244	0.248	2.016	0.000098
(11,0)ZSWCNTs	0.007	0.377	-0.370	0.354	1.412	0.000069
(6,0)ZSWBNNTs	-0.046	1.226	-1.312	1.289	0.388	0.0054
(7,0)ZSWBNNTs	0.047	1.688	-1.641	1.665	0.300	0.00066
(11,0)ZSWBNNTs	-0.094	1.984	-2.078	2.031	0.246	0.0021
CY/ (6,0)ZSWCNTs	-	-	-	-	-	-
5-FU/ (7,0)ZSWCNTs	-0.028	0.118	-0.147	0.133	3.759	0.0029
CH/ (11,0)ZSWCNTs	0.036	0.119	-0.154	0.137	3.640	0.0047
CY/ (6,0)ZSWBNNTs	-0.031	1.203	-1.234	1.220	0.409	0.00039
5-FU/ (7,0)ZSWBNNTs	-0.032	1.359	-1.391	1.375	0.364	0.00037
CH/ (11,0)ZSWBNNTs	0.088	0.130	-0.042	0.086	5.814	0.04500

4. Conclusions

We are used DFT method to know the best substrate from ZSWCNTs and ZSWBNNTs can be utilized to deliver (CY, 5-FU, and CH) anticancer drugs in different distance between the anticancer drug and these tubes. We computed various electronic properties of the complex structures (anticancer drug/(ZSWCNTs or ZSWBNNTs)). We detected that the pristine (6,0) ZSWCNTs has a metallic behavior with zero electronic band gap, but the others tubes have semiconductor behaviors. The total energy is increasing by increasing the diameter of the tubes. Then, these tubes become more stable and lower reactive. Results shown that the complex structures have electronic band gap less than the pristine of these tubes. By adsorbing the same anticancer drug on the ZSWCNTs and ZSWBNNTs, we pointed out that the anticancer drug/ZSWBNNTs have interesting results compared with ZSWCNTs. So, the electronic band gap is reduced for complex structures compared with pristine tubes. Also, the anticancer drug/ZSWBNNTs is more stable compared with anticancer drug/ZSWCNTs. In brief, we discovered that the ZSWBNNTs is the greatest substrate to carry these anticancer drugs compared with SWCNTs.

References

- [1] N. Anzar, R. Hasan, M. Tyagi, N. Yadav, and J. Narang, "Carbon nanotube-A review on Synthesis, Properties and plethora of applications in the field of biomedical science," *Sensors International*, vol. 1, p. 100003, 2020.
- [2] F. N. Ajeel, M. H. Mohammed, and A. M. Khudhair, "Effects of lithium impurities on electronic and optical properties of graphene nanoflakes: a DFT-TDDFT study," *Chinese Journal of Physics*, vol. 58, pp. 109-116, 2019.
- [3] V. Khodadadi, N. Hasanzadeh, H. Yahyaei, and A. Rayatzadeh, "A QUANTUM MECHANICS AND MOLECULAR MECHANICS STUDY OF THE EFFECTS OF DIFFERENT SOLVENTS AND TEMPERATURES ON THE CONNECTIONS OF METHOTREXATE DERIVATIVES ANTICANCER DRUG TO NANOTUBES CARRIERS," *Journal of the Chilean Chemical Society*, vol. 66, no. 4, pp. 5365-5379, 2021.
- [4] M. Rahamathulla *et al.*, "Carbon nanotubes: Current perspectives on diverse applications in targeted drug delivery and therapies," *Materials*, vol. 14, no. 21, p. 6707, 2021.
- [5] R. Dubey, D. Dutta, A. Sarkar, and P. Chattopadhyay, "Functionalized carbon nanotubes: Synthesis, properties and applications in water purification, drug delivery, and material and biomedical sciences," *Nanoscale Advances*, vol. 3, no. 20, pp. 5722-5744, 2021.
- [6] M. Mehrmohamadi, S. H. Jeong, and J. W. Locasale, "Molecular features that predict the response to antimetabolite chemotherapies," *Cancer & metabolism*, vol. 5, no. 1, p. 8, 2017.
- [7] K. Shayan and A. Nowroozi, "Boron nitride nanotubes for delivery of 5-fluorouracil as anticancer drug: a theoretical study," *Applied Surface Science*, vol. 428, pp. 500-513, 2018.
- [8] S. Viaud *et al.*, "The intestinal microbiota modulates the anticancer immune effects of cyclophosphamide," *science*, vol. 342, no. 6161, pp. 971-976, 2013.
- [9] A. Iqbal *et al.*, "Molecular mechanism involved in cyclophosphamide-induced cardiotoxicity: Old drug with a new vision," *Life sciences*, vol. 218, pp. 112-131, 2019.
- [10] H. Araissia *et al.*, "Physico-Chemical Properties of Three Synthesized Carbonaceous Nanomaterials (CNTs, GO, Biochar) for Perspective Application: Water/Soil Treatment and Energy Storage," *Engineering Science*, vol. 3, no. 1, p. 35, 2023.
- [11] M. Zarghami Dehaghani *et al.*, "Theoretical encapsulation of fluorouracil (5-FU) anti-cancer chemotherapy drug into carbon nanotubes (CNT) and boron nitride nanotubes (BNNT)," *Molecules*, vol. 26, no. 16, p. 4920, 2021.
- [12] Z. Es' haggi and F. Moeinpour, "Carbon nanotube/polyurethane modified hollow fiber-pencil graphite electrode for in situ concentration and electrochemical quantification of anticancer drugs Capecitabine and Erlotinib," *Engineering in Life Sciences*, vol. 19, no. 4, pp. 302-314, 2019.
- [13] F. N. Ajeel, M. H. Mohammed, and A. M. Khudhair, "Electronic, thermochemistry and vibrational properties for single-walled carbon nanotubes," *Nanoscience & Nanotechnology-Asia*, vol. 8, no. 2, pp. 233-239, 2018.
- [14] A. M. Khudhair and A. Ben Ahmed, "Pure and Stone-Wales Defect Armchair Boron Nitride Graphene Nanoribbons as Anticancer Drug Delivery Vehicles: A Theoretical Investigation," *Journal of Cluster Science*, vol. 35, no. 2, pp. 451-460, 2024.
- [15] F. Nimr Ajeel, A. Mohsin Khuodhair, and S. Mahdi AbdulMohsin, "Improvement of the optoelectronic properties of organic molecules for nanoelectronics and solar cells applications: via DFT-B3LYP investigations," *Current Physical Chemistry*, vol. 7, no. 1, pp. 39-46, 2017.

- [16] F. N. Ajeel, M. H. Mohammed, and A. M. Khudhair, "Tuning the electronic properties of the fullerene C 20 cage via silicon impurities," *Russian Journal of Physical Chemistry B*, vol. 11, pp. 850-858, 2017.
- [17] A. M. Khudhair, F. N. Ajeel, and M. H. Mohammed, "Theoretical study of the electronic and optical properties to design dye-sensitivity for using in solar cell device," *Russian Journal of Physical Chemistry B*, vol. 12, pp. 645-650, 2018.
- [18] A. M. Khudhair, M. H. Mohammed, F. N. Ajeel, and S. H. Mohammed, "Enhancement the electronic and optical properties of the graphene nanoflakes in the present S impurities," *Chemical Physics Impact*, vol. 6, p. 100154, 2023.
- [19] M. H. Mohammed, F. N. Ajeel, and A. M. Khudhair, "Analysis the electronic properties of the zigzag and armchair single wall boron nitride nanotubes with single Li impurity in the various sites," *Journal of Electron Spectroscopy and Related Phenomena*, vol. 228, pp. 20-24, 2018.
- [20] M. Hesabi and R. Behjatmanesh-Ardakani, "Interaction between anti-cancer drug hydroxycarbamide and boron nitride nanotube: a long-range corrected DFT study," *Computational and Theoretical Chemistry*, vol. 1117, pp. 61-80, 2017.
- [21] F. N. Ajeel, M. H. Mohammed, and A. M. Khudhair, "SWCNT as a model nanosensor for associated petroleum gas molecules: via DFT/B3LYP investigations," *Russian Journal of Physical Chemistry B*, vol. 13, pp. 196-204, 2019.
- [22] F. N. Ajeel, "Engineering electronic structure of a fullerene C20 bowl with germanium impurities," *Chinese Journal of Physics*, vol. 55, no. 5, pp. 2134-2143, 2017.
- [23] A. M. Khudhair, F. N. Ajeel, and M. H. Mohammed, "Theoretical (DFT and TDDFT) insights into the effect of polycyclic aromatic hydrocarbons on Monascus pigments and its implication as a photosensitizer for dye-sensitized solar cells," *Microelectronic Engineering*, vol. 212, pp. 21-26, 2019.
- [24] A. M. Khudhair, K. H. Bardan, A. Almusawe, and F. N. Ajeel, "Enhancement the electronic and optical properties for the dye Disperse Orange 13 and using in the solar cell device," in *IOP Conference Series: Materials Science and Engineering*, 2020, vol. 928, no. 7: IOP Publishing, p. 072031.
- [25] M. K. Hommod and L. F. Auqla, "Density Functional Theory Investigation For Ni6, Co5, Au12, Y5 and Ni6Li, Co5Li, Au12Li, Y5Na Interactions," *University of Thi-Qar Journal of Science*, vol. 9, no. 2, pp. 105-112, 2022.
- [26] M. N. Mutier and L. F. Al-Badry, "Effect of Direct Coupling on Electronic Transport and Thermoelectric Properties of Single Pyrene Molecule," *University of Thi-Qar Journal of Science*, vol. 8, no. 2, pp. 94-99, 2021.
- [27] M. H. Mohammed, F. N. Ajeel, S. H. Mohammed, A. M. Khudhair, and F. H. Hanoon, "Engineering and controlling the electronic properties of zigzag and armchair boron nitride nanotubes with various concentrations of oxygen impurities," *Chinese Journal of Physics*, vol. 89, pp. 793-800, 2024.
- [28] A. M. Khudhair and A. B. Ahmed, "Utilizing circumcoronene and BN circumcoronene for the delivery and adsorption of the anticancer drug floxuridine," *Computational and Theoretical Chemistry*, vol. 1222, p. 114075, 2023.
- [29] A. M. Khudhair, A. B. Ahmed, F. N. Ajeel, and M. H. Mohammed, "Theoretical investigation on the therapeutic applications of C2B and C2O as targeted drug delivery systems for hydroxyurea and 6-thioguanine in cancer treatment," *Nano-Structures & Nano-Objects*, vol. 38, p. 101135, 2024.

- [30] A. M. Khudhair and A. Ben Ahmed, "Anticancer drugs delivery and adsorption computations in pure and Stone–Wales defect armchair graphene nanoribbons," *Optical and Quantum Electronics*, vol. 55, no. 9, p. 812, 2023.
- [31] A. M. Khudhair and A. Ben Ahmed, "Adsorption Characteristics of the Anticancer Drug Hydroxyurea with Armchair BN Graphene Nanoribbons Containing and Lacking Vacancy Defects: Insight via DFT Calculations," *Journal of Superconductivity and Novel Magnetism*, pp. 1-10, 2024.
- [32] F. N. Ajeel, K. H. Bardan, S. H. Kareem, and A. M. Khudhair, "Pd doped carbon nanotubes as a drug carrier for Gemcitabine anticancer drug: DFT studies," *Chemical Physics Impact*, vol. 7, p. 100298, 2023.
- [33] T. A. Omeer and M. H. Mohammed, "Effective and controlling on the electronic properties of the graphene nanoflakes in the presents various concentrations of the B, N, and O impurities," 2023.
- [34] M. H. Mohammed and F. H. Hanoon, "Application of zinc oxide nanosheet in various anticancer drugs delivery: quantum chemical study," *Inorganic Chemistry Communications*, vol. 127, p. 108522, 2021.
- [35] V. Jindal and A. N. Imtani, "Bond lengths of armchair single-waled carbon nanotubes and their pressure dependence," *Computational materials science*, vol. 44, no. 1, pp. 156-162, 2008.
- [36] M. H. Mohammed, A. S. Al-Asadi, and F. H. Hanoon, "Electronic structure and band gap engineering of bilayer graphene nanoflakes in the presence of nitrogen, boron and boron nitride impurities," *Superlattices and Microstructures*, vol. 129, pp. 14-19, 2019.
- [37] J.-C. Charlier, X. Blase, and S. Roche, "Electronic and transport properties of nanotubes," *Reviews of modern physics*, vol. 79, no. 2, p. 677, 2007.
- [38] C. L. Kane and E. Mele, "Size, shape, and low energy electronic structure of carbon nanotubes," *Physical Review Letters*, vol. 78, no. 10, p. 1932, 1997.
- [39] T. W. Odom, J.-L. Huang, P. Kim, and C. M. Lieber, "Structure and electronic properties of carbon nanotubes," vol. 104, ed: ACS Publications, 2000, pp. 2794-2809.
- [40] Y. Matsuda, J. Tahir-Kheli, and W. A. Goddard III, "Definitive band gaps for single-wall carbon nanotubes," *The Journal of Physical Chemistry Letters*, vol. 1, no. 19, pp. 2946-2950, 2010.
- [41] E. Tetik, F. Karadağ, M. Karaaslan, and İ. Çömez, "The electronic properties of the graphene and carbon nanotubes: ab initio density functional theory investigation," *International Scholarly Research Notices*, vol. 2012, 2012.
- [42] G. Kim, J. Bernholc, and Y.-K. Kwon, "Band gap control of small bundles of carbon nanotubes using applied electric fields: A density functional theory study," *Applied Physics Letters*, vol. 97, no. 6, 2010.
- [43] F. Li, J. Lu, G. Tan, M. Ma, X. Wang, and H. Zhu, "Boron nitride nanotubes composed of four-and eight-membered rings," *Physics Letters A*, vol. 383, no. 1, pp. 76-82, 2019.